

Article

# Evaluation of Hydraulic Performance Characteristics of a Newly Designed Dynamic Fluidic Sprinkler

Xingye Zhu <sup>1</sup>, Alexander Fordjour <sup>1,2</sup>, Shouqi Yuan <sup>1</sup>, Frank Dwomoh <sup>2</sup> and Daoxing Ye <sup>3,\*</sup>

<sup>1</sup> Research Centre of Fluid Machinery Engineering and Technology, Jiangsu University, Zhenjiang 212013, China; zhuxy@ujs.edu.cn (X.Z.); fordjouralexander27@yahoo.com (A.F.); shouqiy@ujs.edu.cn (S.Y.)

<sup>2</sup> Department of Civil Engineering, Koforidua Technical University, Koforidua P.O.BOX KF 981, Ghana; agyenfrank@yahoo.com

<sup>3</sup> Key Laboratory of Fluid and Power Machinery, Xihua University, Chengdu 610039, China

\* Correspondence: dxingye@163.com

Received: 29 August 2018; Accepted: 18 September 2018; Published: 21 September 2018



**Abstract:** A newly designed dynamic fluidic sprinkler was tested with different types of nozzles at different operating pressures. Therefore, the aim of this paper was to evaluate the hydraulic performance of a newly designed dynamic fluidic sprinkler. MATLAB R2014a software was employed to establish the computational program for the computed uniformity. Droplet sizes were determined using a Thies Clima Laser Precipitation Monitor. Results showed that the nozzle with a diameter of 5.5 mm gave the highest coefficient of uniformity value of 86% at a low pressure of 150 kPa. The comparison of water distribution profiles for the nozzle sizes (2, 3, 4, 5.5, 6 and 7 mm) at different operating pressures (100, 150, 200, 250 and 300 kPa) showed that a 5.5-mm nozzle size produced a parabola-shaped profile at 150 kPa. The mean droplet diameters for the nozzles sizes of 2, 3, 4, 5.5, 6 and 7 mm ranged from 0 to 4.2, 0 to 3.7, 0 to 3.6, 0 to 3.2, 0 to 0.5 and 0 to 3.8 mm, respectively. The comparison of droplet size distributions showed that 5.5 mm had the optimum droplet diameter of 3.2 mm. The largest droplet sizes had a maximum value of 4.0 for a 2-mm nozzle size. For all the nozzles sizes, 5.5 mm produced better results for hydraulic performance, which can significantly improve the performance and save water for crop production in sprinkler-irrigated fields.

**Keywords:** sprinkler irrigation; dynamic fluidic sprinkler; droplet size; uniformity coefficient; water distribution; nozzles

## 1. Introduction

Sprinkler irrigation technology has been widely used especially in agriculture to save water. It has great potential for improving the water use efficiency of crops. Furthermore, the irrigation engineer can control the amount of water applied, and it is more easily scheduled, which can increase water productivity per the unit of water consumed [1,2]. The sprinkler irrigation system distributes water in the form of discrete drops travelling through the air [3]. Sprinkler irrigation can play a significant role in irrigation development in third world countries, if the system is properly selected, designed and operated. Sprinkler systems have accelerated and been revolutionized with the development of irrigated agriculture in several parts of the world. It is therefore not surprising that the utilization of sprinkler irrigation systems has recently increased [4,5].

According to [6,7], the performance of a sprinkler is determined by its discharge, wetted radius, distribution pattern, application rate and droplet sizes. Water application rate can be defined as the depth of water applied to the area per unit time. It determines which sprinkler should be assigned to a particular soil, crop and terrain on which it operates. The application rate depends on the operating

pressures, the nozzle size and distance between sprinklers [8]. However, the effect of operating pressure on application rate is minimal compared to the effect of the sprinkler nozzle on the application rate [3]. For most sprinklers, when the operating pressure is increased, the discharge tends to balance the increase in wetted area. It has been found that a sprinkler nozzle that produces little droplets covers a smaller wetted area, which also has the highest average application rate. Increasing the nozzle diameter increases the average application rate, since the sprinkler discharge tends to increase more rapidly than wetted area [9]. According to [10,11], the application uniformity of a sprinkler is an important performance criterion for the design and evaluation of sprinklers, which is primarily influenced by operating pressure, sprinkler size and spacing.

Several studies have been conducted to analyze the droplet size distribution with different types of sprinklers over the years. The work in [12] showed that drop size distributions have a direct effect on irrigation water kinetics energy and wind drift. The work in [13] analyzed the droplet size characteristics of a complete fluidic sprinkle and concluded that about 50% of the droplets had a diameter of less 0.5 mm and that 50% of the water volume consisted of droplets with a diameter less than 2 mm at most distances. The work in [14] reported that nozzle size and pressure configurations have an influence on droplet formation. Similarly, [15,16] reported that drop sizes can also influence the design, uniformity and efficiency of irrigation systems. According to [17], wind speed has been found to affect fine drops more than large drops. The work in [18] showed that small drops are subject to large evaporation losses under high vapor pressure. However, when drop evaporation is controlled by air friction, large drops can account for most evaporation losses [19]. The work in [20] reported that drops produced by a sprinkler are subject to several factors; such as the type of sprinkler and nozzle, operating parameters and environmental conditions.

Other researchers have proposed equations to express the coefficient of uniformity [21,22]. The different equations available to express the coefficient of uniformity (CU) are based on some measures of variation in water distribution. The work in [23,24] considered a coefficient of uniformity value of less than 85% as “low” and a CU of 85% or above as “desirable”. According to [25,26], Christiansen’s coefficient of uniformity is the most widely used for water distribution uniformity assessment in sprinkler irrigation.

Over the years, extensive research works have been carried out to improve the structure and efficiency of the fluidic sprinkler for crop production. The work in [27] conducted experiments on drop size distributions and droplet characterization of a complete fluidic sprinkler with different nozzle dimensions. The work in [28] performed a numerical simulation and experimental study on a new type of variable-rate fluidic sprinkler. The work in [29] researched the field performance characteristics of a fluidic sprinkler. The work in [30] compared fluidic and impact sprinklers based on hydraulic performance. The work in [31] analyzed smoothed particle hydrodynamics and its applications in fluid-structure interactions. The work in [32] concluded that variations in quadrant completion times were small for both fluidic and impact sprinklers. However, deviations in water application rate were higher with the fluidic sprinkler. The work in [29] studied the relationship between rotation speed and operating pressure and pointed out that the inner angle of a fluidic sprinkler varied in quite a range among geometrical parameters. Subsequently, the authors concluded that further study needed to be carried out on the design features of the fluidic component. Similarly, Liu et al. [28] carried out a study on the fluidic sprinkler and confirmed the need to optimize the structure.

Only a few studies have focused on improving the rotation of the fluidic sprinkler. However, the rotation instability remains a major difficulty, resulting in the variation of the water application rates. Optimization can enhance the rotation stability and minimize the inconsistency in the water application rates. Therefore, the aim of this paper was to evaluate the hydraulic performance of the newly designed dynamic fluidic sprinkler with different types of nozzles at different operating pressures.

## 2. Materials and Methods

### 2.1. Design of New Dynamic Fluidic Sprinkler Head

In this research, a newly designed dynamic fluidic sprinkler head was manufactured. The following parameters are key factors when it comes to the design of the fluidic structure: the diameter of the main nozzle, the inner contraction angle, the offset length and the working area. The dynamic fluidic sprinkler was developed by Jiangsu University. It is schematically shown in Figure 1. The manufacturing tolerance for the size was  $\pm 0.02$  mm. The main differences between the newly designed dynamic fluidic sprinkler (DFS) and complete fluidic sprinkler (CFS) is the working principle. The newly designed dynamic fluidic sprinkler receives an air signal from a signal tank, but the complete fluidic sprinkler obtains the signal from the fluidic component, found in the working area. When they are operating under a low pressure condition (such as 100 kPa), it is difficult to get the signal flow for the complete fluidic sprinkler. This leads to disappearance of the pressure difference between the two sides of the wall. Therefore, the CFS rotation could not be guaranteed. For the DFS, the air signal flow could be received continuously once the signal tank is filled with water.

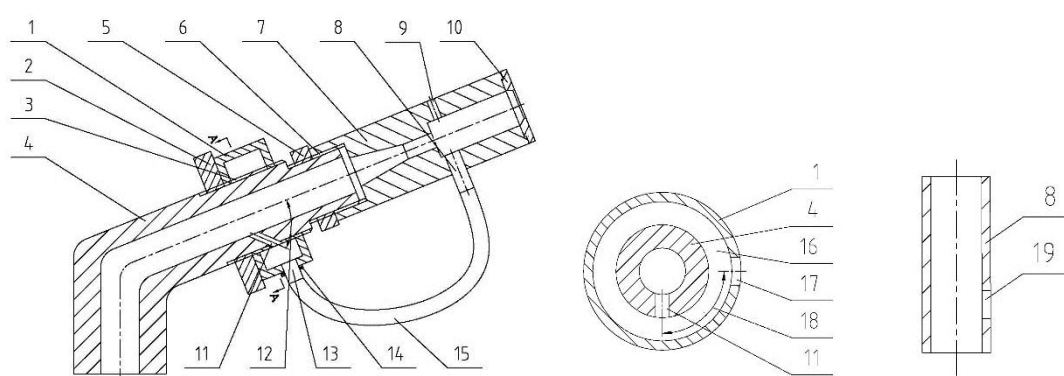


**Figure 1.** Schematic, pictorial view of the new fluidic sprinkler head. 1. Water signal tank. 2. First lock nut. 3. Pipe sprayer. 4. Spray body. 5. Second lock nut. 6. Body of the fluidic element. 7. Jet element body. 8. Water inlet. 9. First air hole. 10. Outlet cover plate. 11. Water dividing hole. 12.  $\alpha$  main flow. 13. Signal nozzle. 14. Third lock nut. 15. Conduit. 16. Water storage capacity. 17. Signal hole. 18.  $\beta$  contraction angle. 19. Second air hole.

### 2.2. Working Principle

The principle of operation of the fluidic sprinkler is based on [33] to perform the function of rotation. Water is ejected from the main nozzle to the working area. A region of low-pressure eddy is formed on both sides of the working area. Air flows into the left side from the reverse blow down nozzle and into the right side from the signal nozzle. The main flow jet is straight because the pressure on both sides is equal and the sprinkler remains stationary, as shown in Figure 2a,b, respectively. The signal flow received from Signal Nozzle 1 fills up Signal Nozzle 2 to transform the right side into a low-pressure eddy. The main flow jet is bent toward the boundary and eventually attached to it because the left pressure is much larger than the right pressure. The phenomenon is repeated step by step, and the sprinkler achieves a stepwise rotation in sequence by self-control. The main flow jet is reattached to the left plane, and the sprinkler rotates to the opposite direction because the right pressure is much larger than the left pressure. The reverse blow down nozzle opens, and air flows into the left side to equalize the pressure again when the sprinkler rotates to the other side. The prototype of the dynamic fluidic sprinkler is shown in Figure 3.

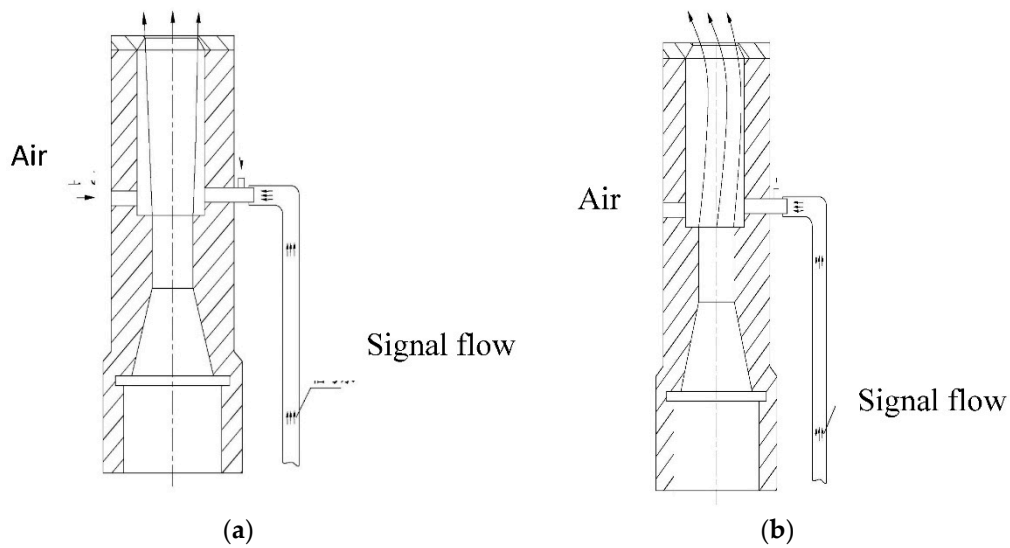


**Figure 2.** (a) Straight main flow jet. (b) Main flow jet reattached to the right.



**Figure 3.** Prototype of the dynamic fluidic sprinkler.

### 2.3. Experimental Procedures

The experiments were conducted at the indoor facilities of the Research Center of Fluid Machinery Engineering and Technology, Jiangsu University (Jiangsu province). The diameter of the circular-shaped indoor laboratory was 44 m. A centrifugal pump was used to supply water from a constant level reservoir. The sprinkler head was mounted on a 1.5-m riser at a 90° angle to the horizontal. Catch cans used in performing the experiments were cylindrical in shape, 200 mm in diameter and 600 mm in height. The catch cans were arranged in two legs around the sprinkler as shown in Figure 4. Each leg contained 14 catch cans placed 1 m apart constituting 28 catch cans in total. The sprinkler was run for some minutes to standardize the environment conditions before the experiment was carried out. The sprinkler flow rate was 4.75 m<sup>3</sup>/h for an operating pressure of 250 kPa, which was controlled by pressure regulation. The operating pressure at the base of the sprinkler head was regulated and maintained by a valve with the aid of a pressure gauge with an accuracy of ±1%. The corresponding operating pressures were 100, 150, 200, 250 and 300 kPa, respectively. The application of water depth measurements was carried out in accordance with [31].



**Figure 4.** Experimental setup in the indoor laboratory.

The experiment lasted for an hour, and the water depth in the catch cans was measured with a graduated measuring cylinder. Droplet sizes were determined using a Thies Clima Laser Precipitation Monitor (TCLPM). It has the following specification: the drop diameter measurement ranges from 0.125 to 8.5 mm in increments of 0.125 mm, and the measuring area is 228 mm long, 200 mm wide with a thickness of 0.75 mm, manufactured by Adolf Thies GMBH & CO.KG, Gottingen, Germany. The principle of operation is such that a beam of light is produced from a laser-optical source in the form of infrared, 785 nm. A photo-diode with a lens is located on the receiver side to determine the optical intensity after transformation into electrical signals. The receiving signal reduces when the water droplet falls through the measuring area. The diameter of the droplet is estimated from the amplitude of the reduction, the droplet velocity of which is calculated from the duration of the reduced signal. For each operating pressure, the droplet size distributions were determined at an interval of 2 m along a radial transect at a distance of 2 m from the sprinkler. For each droplet measurement, the sprinkler was allowed to rotate over the TCLPM at least five times to ensure a sufficient number of drops passed through the measured area. At each pressure, a minimum of three replication assessments were made, and the averaged data were used for the final experiments. Data were ordered according to the drop diameter.

#### 2.4. Computed Coefficient of Uniformity

Matrix Laboratory (MATLAB R2014a) software manufactured by Mathwork Incorporation, Springfield, MA, USA was employed to establish a computational program for the CU. The work in [25,26] reported that Christiansen's coefficient of uniformity is the most widely used and accepted uniformity criterion. Therefore Christiansen's equation was utilized to determine CU.

$$CU = \left( 1 - \frac{\sum_{i=1}^n |X_i - \mu|}{\sum_{i=1}^n X_i} \right) 100\% \quad (1)$$

where  $n$  = number of catch cans;  $x_i$  = measured application depth, mm;  $\mu$  = mean average depth, mm; and  $CU$  = coefficient off uniformity, %.

The model for converting radial data into the net data's insert function was established as follows: Point A is the net point between two adjacent radial rays, and  $(X_k, Y_k)$  is its coordinate.  $P_1, P_2, P_3$  and  $P_4$  are the four nearest points to Point A on the adjacent radial rays, and  $(P_1Q_1), (P_2Q_2), (P_3Q_3)$  and  $(P_4Q_4)$  are their coordinates. Their positions are therefore  $x_1 = P_1 \cos \varnothing_1, (i = 1, 2, 3, 4)$  and  $y_1 = P_1 \sin \varnothing_1, (i = 1, 2, 3, 4)$ ; their water depths are  $h_1, h_2, h_3$  and  $h_4$ ; and the distances away from Point A are  $r_1, r_2, r_3$  and  $r_4$ , respectively. Thus,

$$r_1 = \sqrt{(X_i - X_k)^2 + (Y_i - Y_k)^2} (i = 1, 2, 3, 4) \quad (2)$$

The water depth A can be expressed as:

$$h_A = C_1 h_1 + C_2 h_2 + C_3 h_3 + C_4 h_4 \quad (3)$$

where:

$$C_1 = (r_2 r_3 r_4)^2 / R, C_2 = (r_1 r_3 r_4)^2 / R, C_3 = (r_1 r_2 r_4)^2 / R, C_4 = (r_1 r_2 r_3)^2 / R, \quad (4)$$

$$R = (r_1 r_2 r_3)^2 + (r_1 r_3 r_4)^2 + (r_1 r_2 r_4)^2 + (r_2 r_3 r_4)^2 \quad (5)$$

According to the actual measurements, the water depth of every point can be calculated using Equation (2). The combined coefficient of uniformity can then be calculated for the overlapping of the spray sprinkler with different lateral spacings.

Basic drop statistics: Managing the large dataset obtained from the photographs required a statistical approach. While it is convenient to represent the sets by a reduced number of parameters, some traits of the drop populations can be obscured by the choice of statistical parameters. The parameters used in this work for drop diameter included arithmetic mean diameter (Equation (6)), standard deviation (Equation (8)) and coefficient of variation (Equation (9)). The following addition parameters were determined for drop diameter: the volumetric mean ( $D_v$ ) and average volumetric diameter ( $D_{50}$ ).

$$\bar{d} = \frac{\sum_{i=1}^n m_i d_i}{\sum_{i=1}^n m_i} \quad (6)$$

$$d_v = \frac{\sum_{i=1}^n d_i^4}{\sum_{i=1}^n d_i^3} \quad (7)$$

$$SD_D = \sqrt{\frac{1}{n-1} \sum_{i=1}^n (d_i - \bar{d})^2} \quad (8)$$

$$CV_D = \left( \frac{SD_D}{\bar{d}} \right) \times 100 \quad (9)$$

where  $d_i$  = the diameter of the droplet in each set (mm),  $n_i$  = the droplet number,  $i$  = the number of droplets in the set,  $\bar{d}$  = the arithmetic mean droplet,  $d_v$  = the volume weighted average droplet diameter,  $SD_D$  = the standard deviation and  $CV_D$  = the coefficient of variation.

In order to test the difference between the means of the independent samples of 150 and 250 kPa, the study employed an independent sample  $t$ -test where variances were assumed to be equal with the  $t$ -test statistics formulated as:

$$t = \frac{(\bar{X}_1 - \bar{X}_2) - (\mu_1 - \mu_2)}{\sqrt{\frac{s_1^2}{n_1} + \frac{s_2^2}{n_2}}} \quad (10)$$

where  $\bar{x}_1$  and  $\bar{x}_2$  are sample means,  $\mu_1, \mu_2$  are population means,  $s_1^2$  and  $s_2^2$  are variances and  $n_1$  and  $n_2$  are the sample sizes for 150 and 250kPa, respectively.

The above tests were carried out according to the standards of [34].

### 3. Results and Discussion

As shown in Table 1, the smallest radius of throw was obtained when the sprinkler was operated at the pressure of 100 kPa, and the maximum radius of throw was also obtained at 250 kPa for five of the six nozzles sizes tested in the present experiment. The difference between the maximum and the

minimum radius of throw was 7.2 m. For all the nozzle sizes, the distance of throw increased with an increase in operating pressure until it reached 250 kPa, when it began to decrease. The distance of throw increased when the diameters of the nozzle sizes were increased, and it began to decrease for all the nozzle sizes. Similar findings were reported by [35]. This is possible because at a high pressure condition, the jet breaks up quickly, resulting in smaller radius of throw. For smaller diameters, the jet flow was restricted, resulting in a smaller radius of throw. The result from the independent sample *t*-test analysis (Table 2) showed that there was no significant different between radius of throw for 250 and 150 kPa since ( $p > 0.05$ ). The obtained results for the radius of throw were similar to previous findings by Zhu et al. (2012)

**Table 1.** Radius of throw for different types of nozzles and pressures.

Nozzle Size (mm)	<i>p</i>	Radius of Throw (m)					Standard Deviation				
		100	150	200	250	300	100	150	200	250	300
2		6.4	7.4	7.9	8.7	8.1	0.2 m	0.3 m	0.5 m	0.3 m	0.7 m
3		8.5	9.7	10.7	11.7	10.7	1.2 m	0.1 m	0.6 m	0.2 m	0.4 m
4		11.3	12.4	13.1	12.8	11.5	0.2 m	0.1 m	0.2 m	0.1 m	0.2 m
5.5		10.3	13.3	13.5	13.6	12.5	0.3 m	0.2 m	0.1 m	0.1 m	0.2 m
6		6.4	6.9	7.5	8.2	7.2	0.1 m	0.4 m	0.2 m	0.3 m	0.1 m
7		5.3	6.3	7.4	8.4	7.5	0.1 m	0.2 m	0.4 m	0.5 m	0.4 m

**Table 2.** Independent sample *t*-test.

		Levene’s Test for Equality of Variances		<i>t</i> -Test for Equality of Means					95% Confidence Interval of the Difference	
		F	Sig.	<i>t</i>	df	Sig. (2-tailed)	Mean Difference	Std. Error Difference	Lower	Upper
		Distance	Equal variances assumed	0.727	0.442	−2.530	4	0.065	−0.26667	0.10541
	Equal variances not assumed			−2.530	3.448	0.075	−0.26667	0.10541	−0.57876	0.04542

3.1. Comparison of Water Distribution Profiles

Figure 5 shows the application rate profiles of the newly designed dynamic fluidic sprinkler with different types of nozzles at 100, 150, 200 250 and 300 kPa, respectively. Generally, the application rates increased with an increase in nozzle diameters for all operating pressures, and these results are in agreement with [30]. As the distance from the sprinkler increased, the application rate also increased until it got to the maximum value and decreased for all the pressures. As operating pressure was increased, the application rates increased until they reached the maximum, when they started to decrease. The application rate of the 5.5-mm nozzle varied from 5.24 to 7.42 mm h<sup>−1</sup>. The maximum value of the application rate was obtained for the five analyzed pressures (7.6 mm h<sup>−1</sup> at distances of 8 m for 100 kPa, 6.1 mm h<sup>−1</sup> at 10 m for 150 kPa, 6.23 mm h<sup>−1</sup> at 7 m for 200 kPa, 6.53 mm h<sup>−1</sup> at 7 m for 250 kPa and 7.42 mm h<sup>−1</sup> at 7 m for 300 kPa). Among the pressures, 200 kPa performed slight better than 150 kPa. The result from independent sample *t*-test analysis indicated that there was no significant difference between 250 and 150 kPa ( $p > 0.05$ ). The comparison of the water distribution profiles at different operating pressures showed that all the different nozzle sizes produced parabola-shaped

profiles, but the 5.5-mm nozzle size was flatter than the other nozzle sizes at a low pressure of 150 kPa. This could be attributed to the fact that flow rate at the same operating pressures was much higher and the internal turbulent flow was less uniform from the nozzle outlet, as well as more water was applied near the sprinkler, resulting in a more uniform water distribution for the 5.5-mm nozzle compared to the others. Several studies have shown that [36,37] a doughnut-shaped water distribution leads to surface runoff because more water is deposited away from the sprinkler, affecting the quality of sprinkler irrigation. This implies that a 5.5-mm nozzle size can improve the non-uniform water distribution and save water for crop production. These results are better than those obtained by earlier researchers who used a similar sprinkler type.

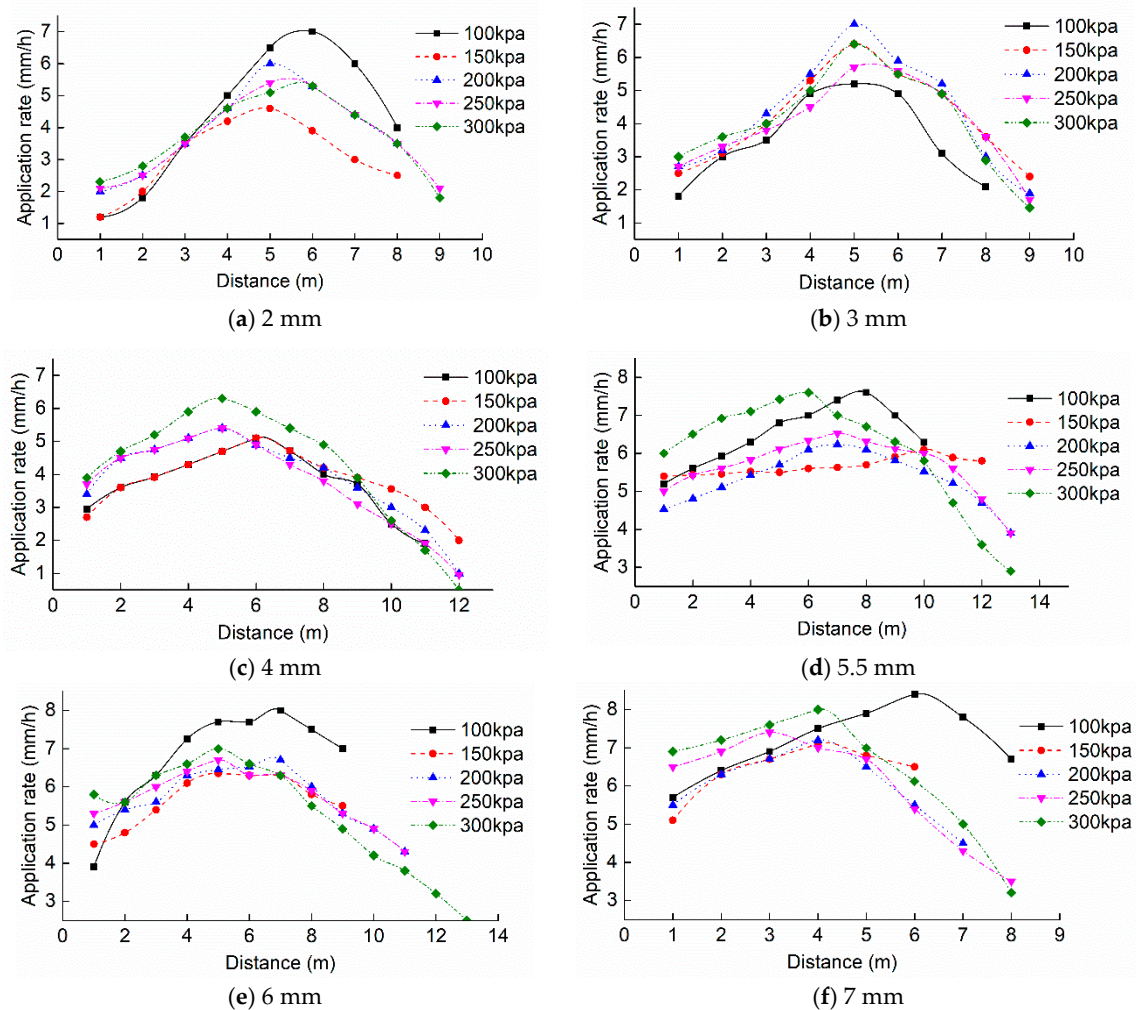
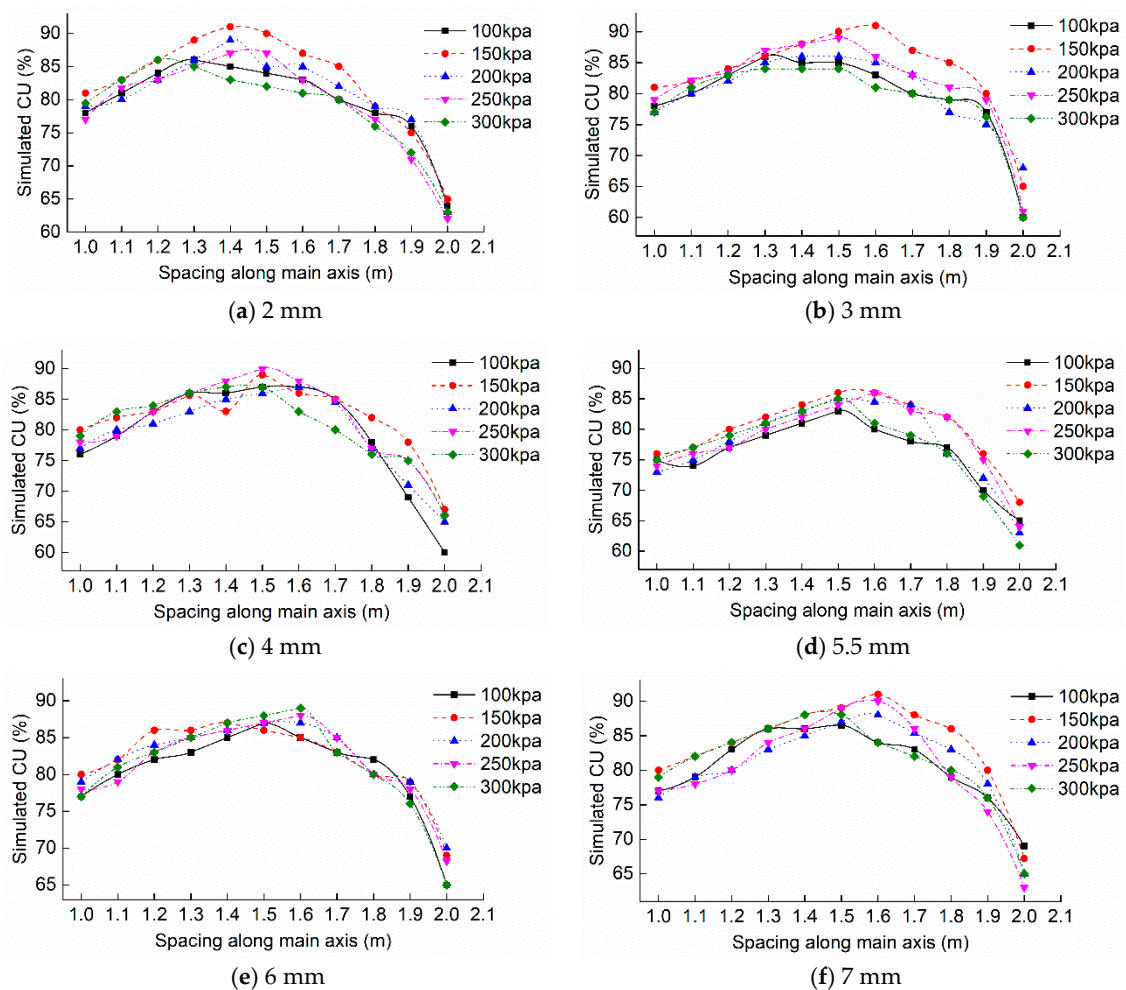


Figure 5. Water distribution profiles for different types of nozzles and pressures.

### 3.2. Comparison of the Computed Uniformity Coefficient

Figure 6 presents the computed coefficients of uniformity with different types of nozzles at 100, 150, 200, 250 and 300 kPa, respectively. The computed coefficients of uniformity were determined using Equation (1). The rectangular spacing for lateral radius times of 1.0, 1.1, 1.2, 1.3, 1.4, 1.5, 1.6, 1.7, 1.8, 1.9 and 2.0 was used for all the nozzle sizes in the study. Figure 6 shows the relationships between the simulated CU and spacing along the vertical and horizontal axis. As the distance from the sprinkler increased, the coefficient of uniformity also increased until it got to the maximum and then decreased for all the pressures and nozzles. The average of the computed values for the 5.5-mm nozzle size was (at different pressures) as follows; 76, 81, 77, 82 and 77% and 100, 150, 200, 250 and 300 kPa, respectively. Comparatively, 250 kPa performed slightly better than 150 kPa, but 150 kPa was selected

as the optimum operating pressure because of rising energy costs. For all the nozzle sizes, 5.5 mm gave the highest computed uniformity value of 86%, at a low pressure of 150 kPa. This indicates that 5.5 mm produced a better water distribution pattern than the rest of the nozzles. These results are slightly better than those obtained by previous researchers for the complete fluidic sprinkler and the outside signals of 82 and 80.88%, respectively [27]. Although 250 kPa gave higher CU than 150, there was no significant difference ( $p > 0.05$ ), along with the increasing cost of energy and growing demand for saving water for optimum crop production. It is appropriate to use 150 kPa.



**Figure 6.** Computed coefficient of uniformity (CU) for different types of nozzles and pressures.

The range of computed CU values for the 5.5-mm nozzle size at 150 kPa was as follows: 77% at a spacing of 1- to 68% at 2.0-times (150 kPa). The highest CU occurred at 1.6-times spacing uniformity and increased with a spacing of one- to 1.6-times, ranging from 76% to 86 with an average of 80%; subsequently, the uniformity decreased with spacing from 1.6- to 2.0-times; the CU value ranged from 84 to 68% with an average of 79.2% at an operating pressure of 150 kPa.

In general, CU values resulting from the 5.5-mm nozzle size were higher compared to other nozzles. The explanation could be that the internal turbulent flow was less uniform from the nozzle outlet and more water was applied near the sprinkler, resulting in a higher combined CU. This supports already established results from earlier research works [24,32,38]. The performance of the tested sprinkler was better than earlier research for the different types of fluidic sprinklers.

### 3.3. Droplet Size Distributions

Figure 7 shows the cumulative droplet diameter frequency for different types of nozzles at different operating pressures. Low operating pressures resulted in larger droplet diameters, and as operating pressures increased, smaller droplets diameters were produced. Droplet diameter increased with distance from the sprinkler for the various nozzle sizes, which is similar to previous results obtained [39].

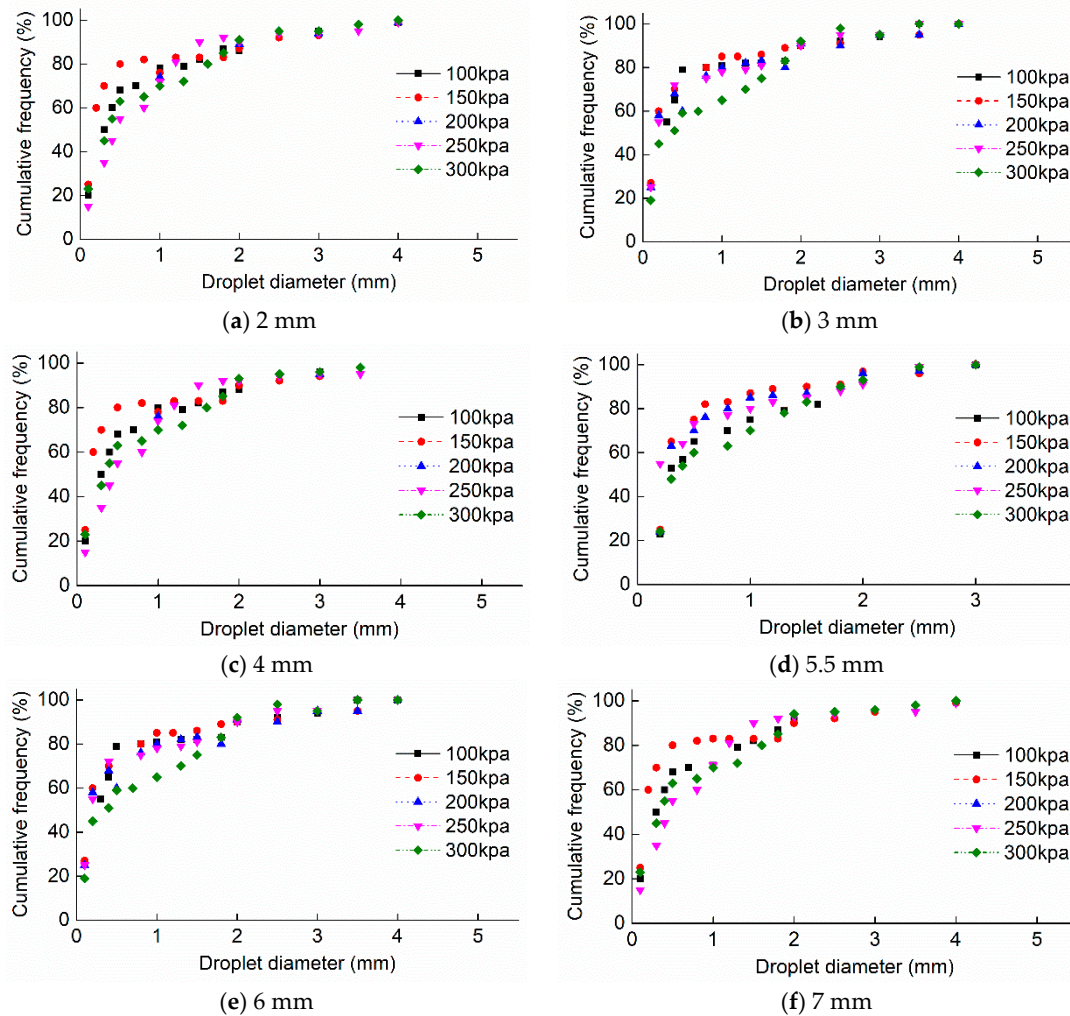


**Figure 7.** Cumulative droplet diameter frequency.

As can be seen in Figure 7, 5.5 mm gave better results than the rest of the nozzles. The average droplet diameters ranged from 0 to 3.2 mm. The cumulative frequencies were under 1 mm of 87, 67, 86.73 and 99%, under 2 mm of 89, 77, 65, 67 and 100% under 3 mm of 88, 90, 67, 88 and 55 at pressures of 100, 150, 200, 250 and 300 kPa, respectively. The mean droplet diameters for the nozzle sizes of 2, 3, 4, 5.5, 6 and 7 mm ranged from 0 to 4.2, 0 to 3.7, 0 to 3.6, 0 to 3.2, 0 to 0.5 and 0 to 3.8 mm, respectively. The comparison of droplet size distributions showed that 5.5 mm had the narrowest droplet size and smallest maximum droplet diameter of 3.2 mm. The biggest droplet size ranged with the maximum value of 4.2 for a nozzle size of 2 mm. These results are similar to those obtained by previous researchers who used different sprinkler types [24,26,35,36]. It can also be noted that at most distances from the sprinkler, the number of droplets at smaller diameters was greater compared to that at larger diameters. This goes to support the hypothesis that droplet formation is a continuous process along the jet trajectory [40–42]. Using a 5.5-mm nozzle size will produce optimum droplet sizes, which can fight wind drift and evaporation losses. This is because large droplets possess high

kinetic energy, and on impact, they disrupt the soil surface, especially soils with crustiness problems, leading to sealing of the soil surface. Dwomoah et al. reported similar results when analyzing drop diameter measurements performed with the Thies Clima Laser Precipitation Monitor (TCLPM).

Table 3 shows the percentage of droplets with a mean diameter for the various nozzle sizes at different operating pressures. Diameters  $d_{10}$ ,  $d_{25}$ ,  $d_{50}$ ,  $d_{75}$  and  $d_{90}$  represent the diameters corresponding to 10, 25, 50, 75 and 90%, respectively, of the volume of detected water. From the table, it can be observed that for all the nozzle sizes, droplet size increased with increasing percentage of droplet diameter. In this experiment, almost 20% of the drops identified at all the distances from the sprinkler were smaller than the minimum diameter obtained from earlier researchers who used similar sprinkler types.

**Table 3.** Droplet sizes (mm) for 10, 25, 50, 75 and 90% ( $d_{10}$ ,  $d_{25}$ ,  $d_{50}$ ,  $d_{75}$  and  $d_{90}$ , respectively) for different types of nozzle.

Nozzles Size	Pressure (kPa)	$d_{10}$	$d_{25}$	$d_{50}$	$d_{75}$	$d_{90}$	Standard Deviation
2 mm	100	0.07	0.18	0.45	0.46	1.94	0.76 m
	150	0.05	0.14	0.36	1.09	1.55	0.65 m
	200	0.08	0.15	0.35	1.08	1.56	0.65 m
	250	0.07	0.16	0.27	1.09	1.85	0.7 m
	300	0.09	0.15	0.25	1.3	1.87	0.87 m
3 mm	100	0.06	0.13	0.36	0.47	2.09	0.83 m
	150	0.07	0.14	0.27	0.79	2.4	0.91 m
	200	0.06	0.15	0.25	0.82	2.3	0.93 m
	250	0.06	0.16	0.27	0.5	2.05	0.82 m
	300	0.09	0.18	0.25	1.49	1.96	0.87 m
4 mm	100	0.08	0.13	0.27	0.4	1.69	0.65 m
	150	0.07	0.15	0.26	0.71	1.88	0.75 m
	200	0.07	0.15	0.26	0.73	1.86	0.74 m
	250	0.08	0.17	0.26	1.02	1.82	0.74 m
	300	0.09	0.6	0.25	1.18	1.7	0.65 m
5.5 mm	100	0.04	0.11	0.34	0.44	2.05	0.69 m
	150	0.04	0.12	0.24	0.77	2.1	0.76 m
	200	0.04	0.12	0.23	0.79	2.1	0.75 m
	250	0.04	0.13	0.23	0.48	2.02	0.76 m
	300	0.05	0.14	0.23	0.47	1.93	0.70 m
6 mm	100	0.04	0.11	0.34	0.44	2.05	0.83 m
	150	0.05	0.12	0.24	0.77	2.1	0.85 m
	200	0.05	0.13	0.23	0.79	2.1	0.85 m
	250	0.05	0.14	0.23	0.48	2.02	0.81 m
	300	0.07	0.14	0.23	1.47	1.93	0.87 m
7 mm	100	0.05	0.16	0.44	0.44	1.92	0.76 m
	150	0.05	0.12	0.34	1.07	1.53	0.65 m
	200	0.07	0.13	0.33	1.06	1.51	0.63 m
	250	0.06	0.14	0.25	1.07	1.82	0.76 m
	300	0.06	0.13	0.23	1.28	1.84	0.80 m

$d_{10}$  = represents 10% of the cumulative droplet frequency;  $d_{25}$  = represents 25% of the cumulative droplet frequency;  $d_{50}$  = represents the mean cumulative droplet frequency;  $d_{75}$  = represents 75% of the cumulative droplet frequency;  $d_{90}$  = represents 90% of the cumulative droplet frequency.

### 3.4. Droplet Characterization Statistics

Table 4 presents statistical parameters for the droplets for different types of nozzle at different operating pressures. Parameters include the arithmetic mean diameter, the volumetric mean diameter, the median diameter, the standard deviation and the coefficient of variation. All the parameters decreased with an increase in operating pressure for the nozzle sizes. All the parameters increased as the nozzle sizes increased for all the operating pressures. The mean droplet diameter and volumetric median diameter decreased with operating pressures for the nozzle sizes. Among the nozzles, 5.5 mm

performed better than the rest of the nozzles. The standard deviation of the droplet diameter ranged from 0.69 to 0.86 with a mean of 0.775, and the coefficient of variation ranged from 91 to 147% with a mean value of 119%.

**Table 4.** Droplet statistical parameter for droplet diameters for different types of nozzles.

Nozzle Size (mm)	Pressure (kPa)	$\bar{d}$	$d_v$	$d_{50}$	$SD_D$	$CV_D$
2	100	0.73	3.12	0.45	0.94 m	119
	150	0.71	2.94	0.36	0.71 m	87
	200	0.70	2.79	0.35	0.81 m	107
	250	0.68	2.68	0.37	0.82 m	124
3	100	0.67	2.71	0.36	0.85 m	116
	150	0.69	2.09	0.27	0.71 m	125
	200	0.60	1.93	0.25	8.0 m	120
	250	0.59	1.68	0.23	0.84 m	114
4	100	0.78	2.81	0.27	0.84 m	107
	150	0.76	2.44	0.26	0.68 m	91
	200	0.73	2.0	0.26	0.71 m	99
	250	0.72	1.91	0.25	0.79 m	120
5.5	100	0.86	2.81	0.34	0.89 m	106
	150	0.77	2.34	0.24	0.68 m	91
	200	0.69	2.25	0.23	0.77 m	114
	250	0.57	2.20	0.21	0.83 m	147
6	100	0.89	2.80	0.37	1.02 m	115
	150	0.76	2.79	0.24	0.99 m	132
	200	0.70	2.19	0.23	0.95 m	136
	250	0.68	1.49	0.23	0.87 m	127
7	100	0.80	2.99	0.44	0.92 m	119
	150	0.79	2.39	0.35	0.67 m	85
	200	0.75	2.21	0.33	0.71 m	106
	250	0.66	1.92	0.25	0.79 m	121

$\bar{d}$  = arithmetic mean droplet;  $d_v$  = the volume weighted average droplet diameter;  $SD_D$  = the standard deviation;  $CV_D$  = is the coefficient of variation.

#### 4. Conclusions

This study evaluated the hydraulic performance of a newly designed dynamic fluidic sprinkler using different types of nozzles at different operating pressures. The following conclusions can be drawn.

- 1 The smallest radius of throw was obtained when the sprinkler was operated at the pressure of 100 kPa, while the maximum radius of throw was obtained when the sprinkler was operated at the pressure of 250 kPa. The distance of throw increased with the increase in diameters of nozzle sizes. However, there was no significant different between the radius of throw for 250 and 150 kPa. With the rising cost of energy, it is appropriate to operate under 150 kPa in order to save water.
- 2 The comparison of water distribution profiles at different operating pressures showed that all the different nozzle sizes produced parabola-shaped profiles, while the 5.5-mm nozzle size was flatter at a low pressure of 150 kPa. This implies that a 5.5-mm nozzle size can improve the non-uniform water distribution and save water for sprinkler-irrigated fields.
- 3 For all the nozzle sizes, 5.5 mm gave the highest computed uniformity value of 86%, at a low pressure of 150 kPa. There was no significant difference between 250 and 150 kPa. Comparatively, the sprinkler with a 5.5-mm nozzle produced a better uniformity, and the average CU obtained was within the acceptable range.

- 4 The mean droplet diameter for the nozzles sizes of 2, 3, 4, 5.5, 6 and 7 mm ranged from 0 to 4.2, 0 to 3.7, 0 to 3.6, 0 to 3.2, 0 to 0.5 and 0 to 3.8 mm, respectively. The comparison of the droplet size distribution for the various sizes showed that 5.5 mm had the optimum droplet diameter of 3.2 mm. The largest droplet size had a maximum value of 4.0 for a 2-mm nozzle size. Hence, using a 5.5 mm nozzle size can produce the optimum droplet sizes, which can minimize losses caused by wind drift and evaporation.

**Author Contributions:** X.Z. was the supervision of this manuscript; A.F. was writing the original draft and making all revisions; S.Y. was providing the funding acquisition; F.D. was doing the literature resources; and D.Y. was conducting the experiment.

**Funding:** This research was funded by the National Key Research and Development Program of China (No. 2016YFC0400202), the Priority Academic Program Development of Jiangsu Higher Education Institutions (PAPD), and the open research subject of the key Laboratory (Research Base) of Fluid and Power of Machinery (Xihua University), Ministry of Education (No. szj 2016-067).

**Acknowledgments:** The authors highly acknowledge the supports from students of the Sprinkler Group of the Research Centre of Fluid Machinery and Engineering, Jiangsu University for assistance in conducting the experiment.

**Conflicts of Interest:** The authors declare no conflict of interest.

## References

1. Kahlown, M.A.; Raof, A.; Zubair, M.; Kemper, W.D. Water use efficiency and economic feasibility of growing rice and wheat with sprinkler irrigation in the Indus Basin of Pakistan. *Agric. Water Manag.* **2007**, *87*, 292–298. [[CrossRef](#)]
2. Montazar, A.; Sadeghi, M. Effects of applied water and sprinkler uniformity on alfalfa growth and hay yield. *Agric. Water Manag.* **2008**, *95*, 1279–1287. [[CrossRef](#)]
3. Kincaid, D.C. Spray drop kinetic energy from irrigation sprinklers. *Trans. ASAF* **1996**, *39*, 847–853. [[CrossRef](#)]
4. Kulkarni, S. Innovative technologies for Water saving in Irrigated Agriculture. *Int. J. Water Resour. Arid Environ.* **2011**, *1*, 226–231.
5. Howell, T.A. Enhancing water use efficiency in irrigated agriculture. *Agronomy J.* **2001**, *93*, 281–289. [[CrossRef](#)]
6. Shin, S.; Bae, S. Simulation of water entry of an elastic wedge using the FDS scheme and HCIB method. *J. Hydrodynamics* **2013**, *25*, 450–458. [[CrossRef](#)]
7. Darko, R.O.; Yuan, S.Q.; Liu, J.P.; Yan, H.F.; Zhu, X.Y. Overview of advances in improving uniformity and water use efficiency of sprinkler irrigation. *Int. J. Agric. Biol. Eng.* **2017**, *10*, 1–15.
8. Liu, J.P.; Zhu, X.Y.; Yuan, S.Q.; Wan, J.H.; Chikangaise, P. Hydraulic performance assessment of sprinkler irrigation with rotating spray plate sprinklers in indoor experiments. *J. Irrig. Drain Eng.* **2018**, *144*. [[CrossRef](#)]
9. Li, J.; Rao, M. Sprinkler water distributions as affected by winter wheat canopy. *Irrig. Sci.* **2000**, *20*, 29–35. [[CrossRef](#)]
10. Tang, L.D.; Yuan, S.Q.; Qiu, Z.P. Development and research status of water turbine for hose reel irrigator. *J. Drain. Irrig. Mach. Eng.* **2018**, *36*, 963–968.
11. Al-Ghobari, H.M. Effect of maintenance on the performance of sprinkler irrigation systems and irrigation water conservation. *Food Sci. Agric. Res. Cent. Res. Bull.* **2006**, *141*, 1–6.
12. Kohl, R.A.; Koh, K.S.; Deboer, D.W. Chemigation drift and volatilization potential. *Appl. Eng. Agric.* **1987**, *3*, 174–177. [[CrossRef](#)]
13. Dwomoh, F.A.; Yuan, S.Q.; Li, H. Sprinkler rotation and water application rate for the newly designed complete fluidic sprinkler and impact sprinkler. *Int. J. Agric. Biol. Eng.* **2014**, *7*, 38–46.
14. Zhu, X.; Chikangaise, P.; Shi, W.; Chen, W.H.; Yuan, S. Review of intelligent sprinkler irrigation technologies for remote autonomous system. *Int. J. Agric. Biol. Eng.* **2018**, *11*, 23–30. [[CrossRef](#)]
15. DeBoer, D.W.; Monnens, M.J.; Kincaid, D.C. Measurement of sprinkler drop size. *Appl. Eng. Agric.* **2001**, *17*, 11–15. [[CrossRef](#)]
16. Kohl, R.A.; Bernuth, R.D.; Heubner, G. Drop size distribution measurement problems using a laser unit. *Trans. ASAE* **1985**, *28*, 190–192. [[CrossRef](#)]

17. Fukui, Y.; Nakanishi, K.; Okamura, S. Computer elevation of sprinkler uniformity. *Irrig. Sci.* **1980**, *2*, 23–32. [[CrossRef](#)]
18. Thompson, A.; Gilley, J.R.; Norman, J.M. Sprinkler water droplet evaporation a plant canopy model. *Trans. ASARE* **1993**, *36*, 743–750. [[CrossRef](#)]
19. Lorenzini, G.; Wrachien, D. Performance assessment of sprinkler irrigation system a new indicator for spray evaporation losses. *J. Int. Comm. Irrig. Drain.* **2005**, *54*, 295–305. [[CrossRef](#)]
20. Bautista, C.; Salvador, R.; Burguete, J. Comparing methodologies for the characterization of water drops emitted by an irrigation sprinkler. *Trans. ASABE* **2009**, *52*, 1493–1504.
21. Wilcox, J.C.; Swailes, G.E. Uniformity of water distribution by some under tree orchard sprinklers. *Sci. Agric.* **1947**, *27*, 565–583.
22. Hart, W.E.; Reynolds, W.N. Analytical design of sprinkler systems. *Trans. Am. Soc. Agric. Eng.* **1965**, *8*, 83–85.
23. Kay, M. *Sprinkler Irrigation Equipment and Practice*; Batsford Limited: London, UK, 1988.
24. Keller, J.; Bliesner, R.D. *Sprinkle and Trickle Irrigation*; Van Nostrand Reinhold Pun: New York, NY, USA, 1990.
25. Xiang, Q.J.; Xu, Z.D.; Chen, C. Experiments on air and water suction capability of 30PY impact sprinkler. *J. Drain. Irrig. Mach. Eng.* **2018**, *36*, 82–87.
26. Karmeli, D. Estimating sprinkler distribution pattern using linear regression. *Trans. ASAE* **1978**, *21*, 682–686. [[CrossRef](#)]
27. Liu, J.P.; Liu, W.Z.; Bao, Y.; Zhang, Q.; Liu, X.F. Drop size distribution experiments of gas-liquid two phase's fluidic sprinkler. *J. Drain. Irrig. Mach. Eng.* **2017**, *35*, 731–736.
28. Liu, J.P.; Yuan, S.Q.; Li, H.; Zhu, X.Y. Numerical simulation and experimental study on a new type variable-rate fluidic sprinkler. *J. Agric. Sci. Technol.* **2013**, *15*, 569–581.
29. Dwomoh, F.A.; Yuan, S.; Hong, L. Field performance characteristics of fluidic sprinkler. *Appl. Eng. Agric.* **2013**, *29*, 529–536.
30. Zhu, X.; Yuan, S.; Jiang, J.; Liu, J.; Liu, X. Comparison of fluidic and impact sprinklers based on hydraulic performance. *Irrig. Sci.* **2015**, *33*, 367–374. [[CrossRef](#)]
31. Zhang, A.M.; Sun, P.N.; Ming, F.R.; Colagrossi, A. Smoothed particle hydrodynamics and its applications in fluid-structure interactions. *J. Hydrodynamics* **2017**, *29*, 187–216. [[CrossRef](#)]
32. Zhu, X.; Yuan, S.; Liu, J. Effect of sprinkler head geometrical parameters on hydraulic performance of fluidic sprinkler. *J. Irrig. Drain. Eng.* **2012**, *138*, 1019–1026. [[CrossRef](#)]
33. Coanda, H. Device For Deflecting a Stream of Elastic Fluid Projected Into an Elastic Fluid. U.S. Patent No. 2,052,869, 1 Spetember 1936.
34. American Society of Biological Engineers. *Procedure for Sprinkler Testing and Performance Reporting*; ASAE S398.1; American Society of Biological Engineers: St. Joseph, MI, USA, 1985.
35. Al-araki, G.Y. *Design and Evaluation of Sprinkler Irrigation System. Doctoral Dissertation*; University of Khartoum: Khartoum, Sudan, 2002.
36. Chen, D.; Wallender, W.W. Droplet size distribution and water application with low-pressure sprinklers. *Trans. ASAE* **1985**, *28*, 511–516. [[CrossRef](#)]
37. Li, J.; Kawano, H.; Yu, K. Droplet size distributions from different shaped sprinkler nozzles. *Trans. ASAE* **1994**, *37*, 1871–1878. [[CrossRef](#)]
38. Tarjuelo, J.M.; Montero, J.; Valiente, M.; Honrubia, F.T.; Ortiz, J. Irrigation uniformity with medium size sprinkler, part I: Characterization of water distribution in no—Wind conditions. *Trans. ASAE* **1999**, *42*, 677–689. [[CrossRef](#)]
39. King, B.A.; Winward, T.W.; Bjorneberg, D.L. Comparison of Sprinkler Droplet Size and Velocity Measurements using a Laser Precipitation Meter and Photographic Method. *Am. Soc. Agric. Biol. Eng.* **2013**, 131594348. [[CrossRef](#)]
40. Sudheera, K.P.; Panda, R.K. Digital image processing for determining drop sizes from irrigation spray nozzles. *Agric. Water Manag.* **2000**, *45*, 159–167. [[CrossRef](#)]

41. Liu, J.; Liu, X.; Zhu, X.; Yuan, S. Droplet characterization of a complete fluidic sprinkler with different nozzle dimensions. *Biosyst. Eng.* **2016**, *148*, 90–100. [[CrossRef](#)]
42. Lu, J.; Cheng, J. Numerical simulation analysis of energy conversion in hydraulic turbine of hose reel irrigator JP75. *J. Drain. Irrig. Mach. Eng.* **2018**, *36*, 448–453.



© 2018 by the authors. Licensee MDPI, Basel, Switzerland. This article is an open access article distributed under the terms and conditions of the Creative Commons Attribution (CC BY) license (<http://creativecommons.org/licenses/by/4.0/>).